Electronic Supplementary Material (ESI) for New Journal of Chemistry.

ELECTRONIC SUPPLEMENTARY INFORMATION

Unusual fluorescent behavior of a heteroleptic Cu(I) complex featuring strong electron donating groups on the diimine ligand

Mireya Santander-Nelli,[1,2*] Luis Sanhueza,[3,4] Daniel Navas,[5] Elena Rossin,[6,7] Mirco Natali,[6] Paulina Dreyse[1,*]

[1]Departamento de Química, Universidad Técnica Federico Santa María, Av. España 1680, Casilla 2390123, Valparaíso, Chile.
[2]Centro Integrativo de Biología y Química Aplicada (CIBQA), Universidad Bernardo O'Higgins, Santiago 8370854, Chile.
[3]Departamento de Ciencias Biológicas y Químicas, Facultad de Recursos Naturales, Universidad Católica de Temuco, Casilla 15-D, Temuco, Chile.
[4]Núcleo de Investigación en Bioproductos y Materiales Avanzados (BioMA), Universidad Católica de Temuco, Av. Rudecindo Ortega 02950 Temuco, Chile.
[5]Departamento de Química, Facultad de Ciencias Naturales, Matemática y del Medio Ambiente, Universidad Tecnológica Metropolitana, Las Palmeras 3360, Ñuñoa, Santiago, 7800003, Chile.
[6]Department of Chemical, Pharmaceutical and Agricultural Sciences (DOCPAS), University of Ferrara, Via L. Borsari 46, 44121 Ferrara, Italy.
[7]Department of Chemical Sciences, University of Padova, Via F. Marzolo 1, 35131, Padova, Italy.

[*]Corresponding authors: Mireya Santander-Nelli (mireya.santander@usm.cl) and Paulina Dreyse (paulina.dreyse@usm.cl)

Table of content

S1. NMR characterizations of N^N$_b$

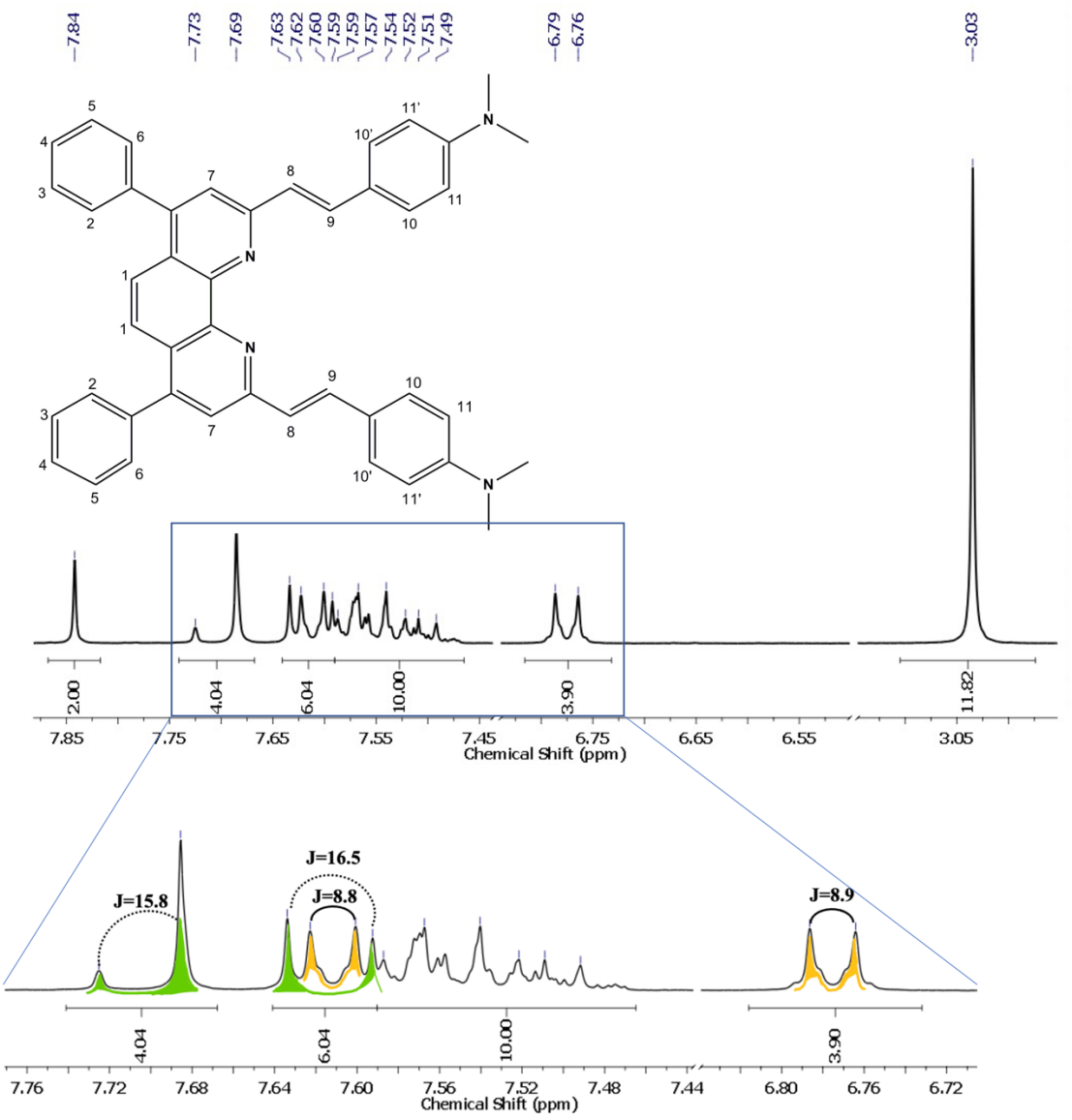

Figure S1. ^{1}H NMR (400 MHz, $CDCl_3$, 298 K) of **N^N$_b$** ligand. Inset shows the hydrogen labels used for the assignation.

^{1}H NMR (400 MHz, $CDCl_3$) δ: 7.84 (s, 2H$_7$), 7.71 (d, $J_{8\text{-}9}$ = 15.8 Hz, 2H$_8$), 7.69 (s, 2H$_1$), 7.61 (d, $J_{9\text{-}8}$ = 16.5 Hz, 2H$_9$), 7.61 (d, $J_{10\text{-}11}$ = 8.8 Hz, 2H$_{10}$, 2H$_{10'}$), 7.59 – 7.49 (m, 2H$_2$, 2H$_3$, 2H$_4$, 2H$_5$, 2H$_6$), 6.78 (d, $J_{11\text{-}10}$ = 8.9 Hz, 2H$_{11}$, 2H$_{11'}$), 3.03 (s, CH_3, 12H).

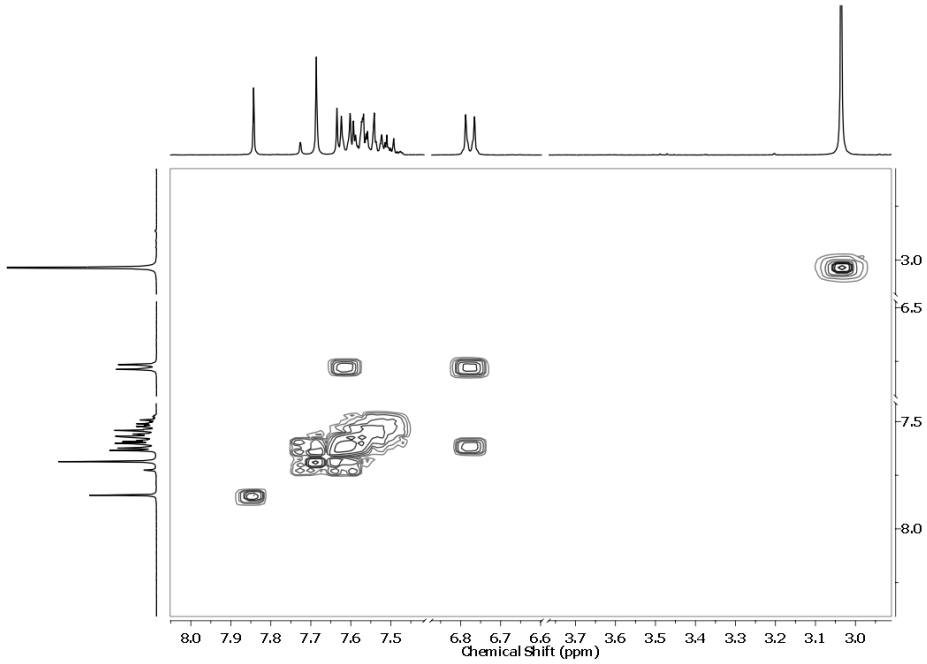

Figure S2. ^{1}H-^{1}H COSY (400 MHz, $CDCl_3$, 298 K) of **N^N$_b$** ligand.

S2. Solubility and stability tests for the Cu (I) complexes studied

S2.1. Evaluation of the solubility

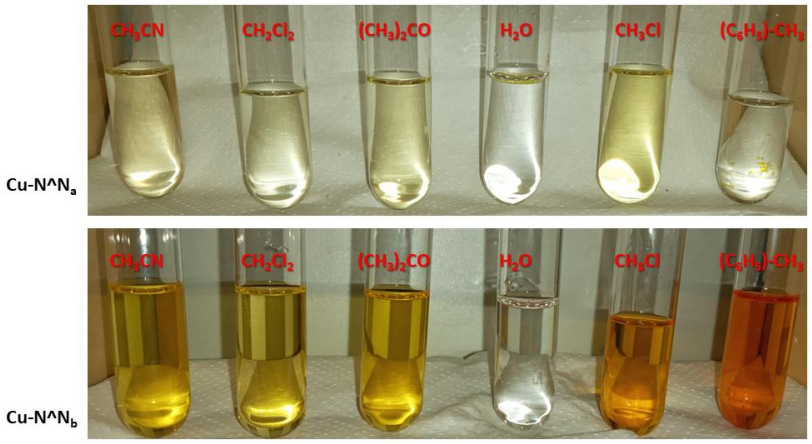

Figure S3. Solubility tests of Cu(I) complexes in acetonitrile, dichloromethane, acetone, water, chloroform and toluene.

S2.2. Evaluation of the stability in coordinating solvent (acetonitrile)

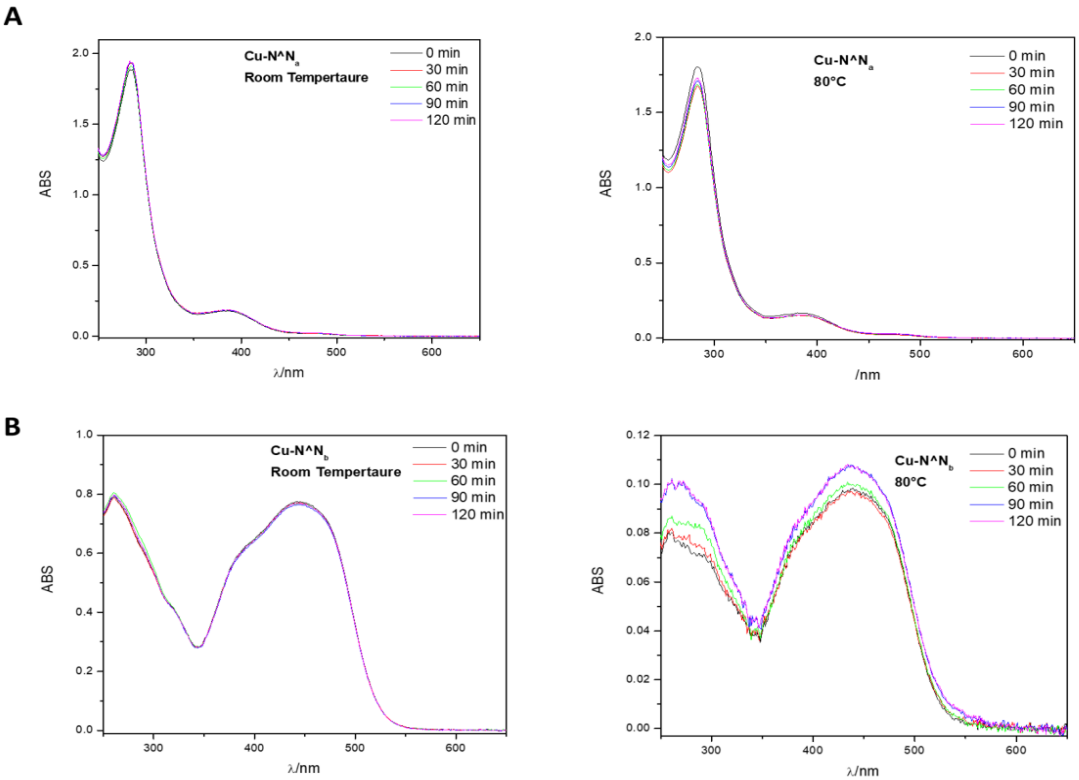

Figure S4. Evaluation of the absorption spectra in time at room temperature and at 80°C for **A.** Cu-N^N$_a$ and **B.** Cu-N^N$_b$.

S3. NMR characterizations of Cu-N^N_a complex

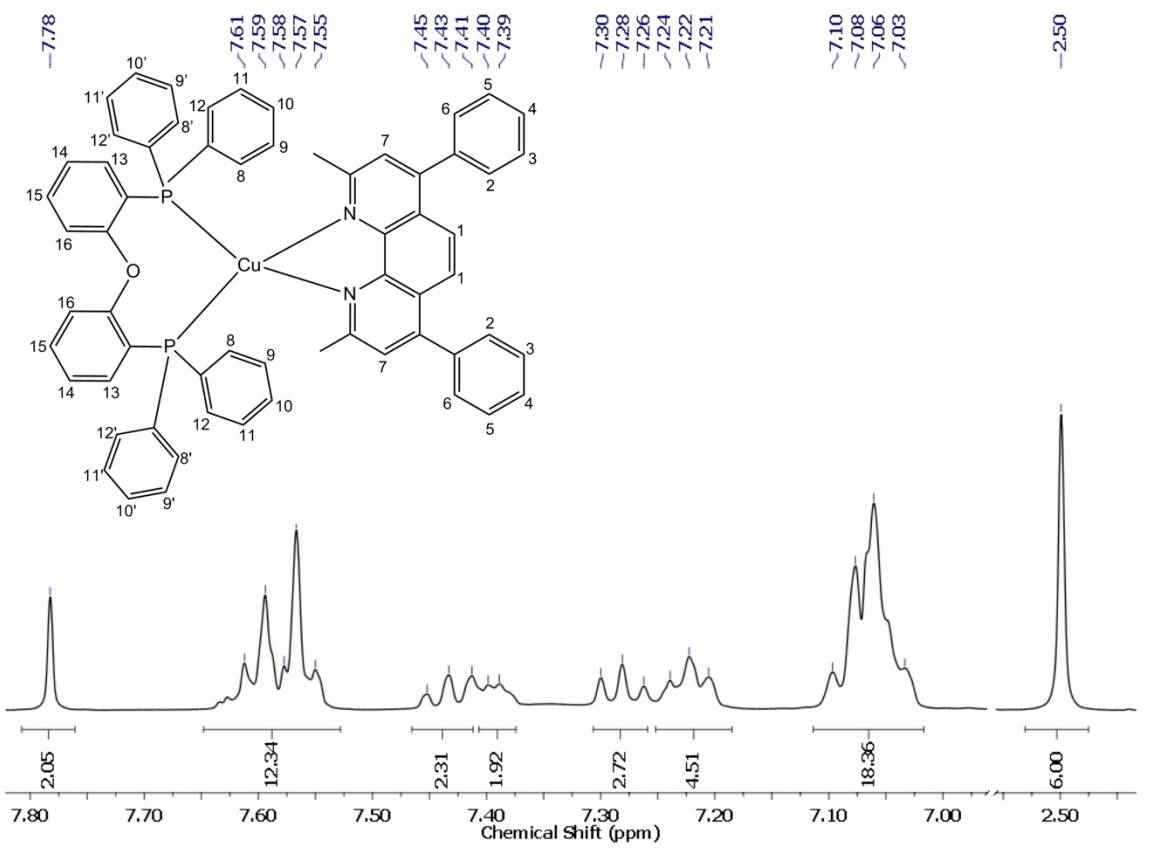

Figure S5. ^{1}H NMR (400 MHz, CD_3CN, 298 K) of **Cu-N^N_a** complex. Inset shows the hydrogen labels used for the assignation.

^{1}H NMR (400 MHz, CD_3CN, 298 K) δ: 7.78 (s, $2H_1$), 7.64 – 7.53 (m, $2H_2$, $2H_3$, $2H_4$, $2H_5$, $2H_6$, $2H_7$), 7.43 (m, $2H_{15}$), 7.39 (m, $2H_{13}$), 7.28 (t, $2H_{14}$), 7.22 (t, $2H_{10}$, $2H_{10'}$), 7.11 – 7.01 (m, $2H_8$, $2H_{8'}$, $2H_9$, $2H_{9'}$, $2H_{11}$, $2H_{11'}$, $2H_{12}$, $2H_{12'}$, $2H_{16}$), 2.50 (s, CH_3, 6H).

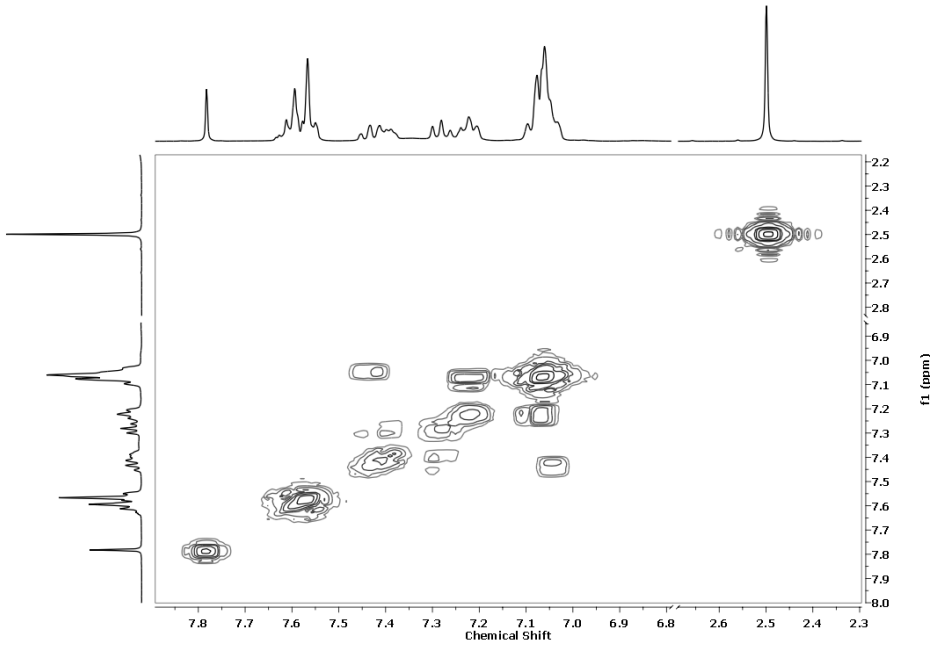

Figure S6. ^{1}H-^{1}H COSY (400 MHz, CD_3CN, 298 K) of **Cu-N^N$_a$** complex.

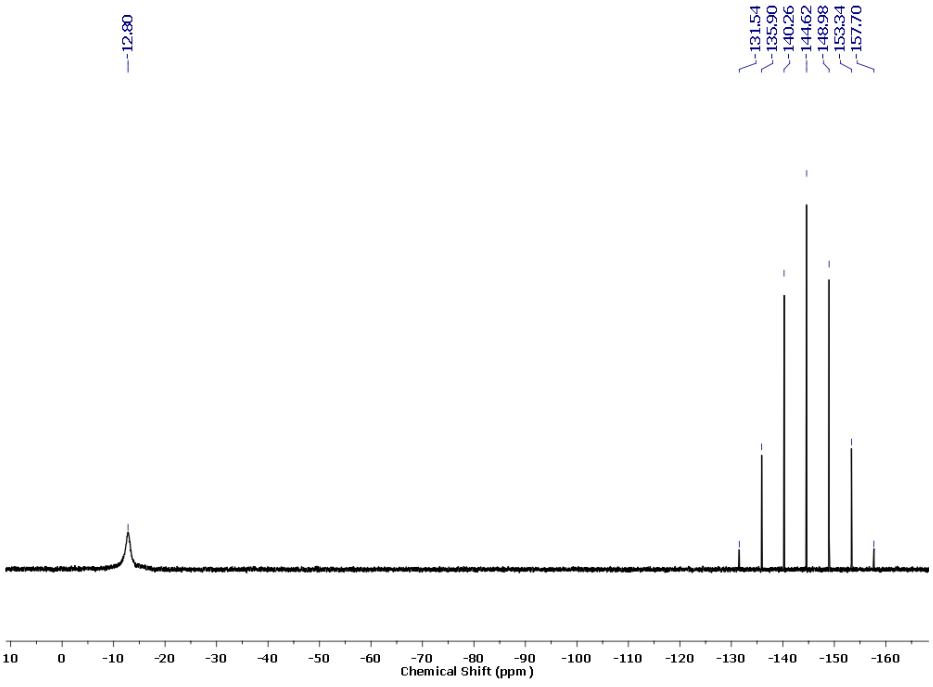

Figure S7. $^{31}P\{^{1}H\}$ NMR (162 MHz, CD_3CN, 298 K) of **Cu-N^N$_a$** complex.

$^{31}P\{^{1}H\}$ NMR (162 MHz, CD_3CN) δ: -12.80 (br s, POP), -144.62 (m, $[PF_6]^-$).

S4. NMR characterizations of Cu-N^N_b complex

S4.1 NMR characterizations of Cu-N^N_b complex in $(CD_3)_2CO$

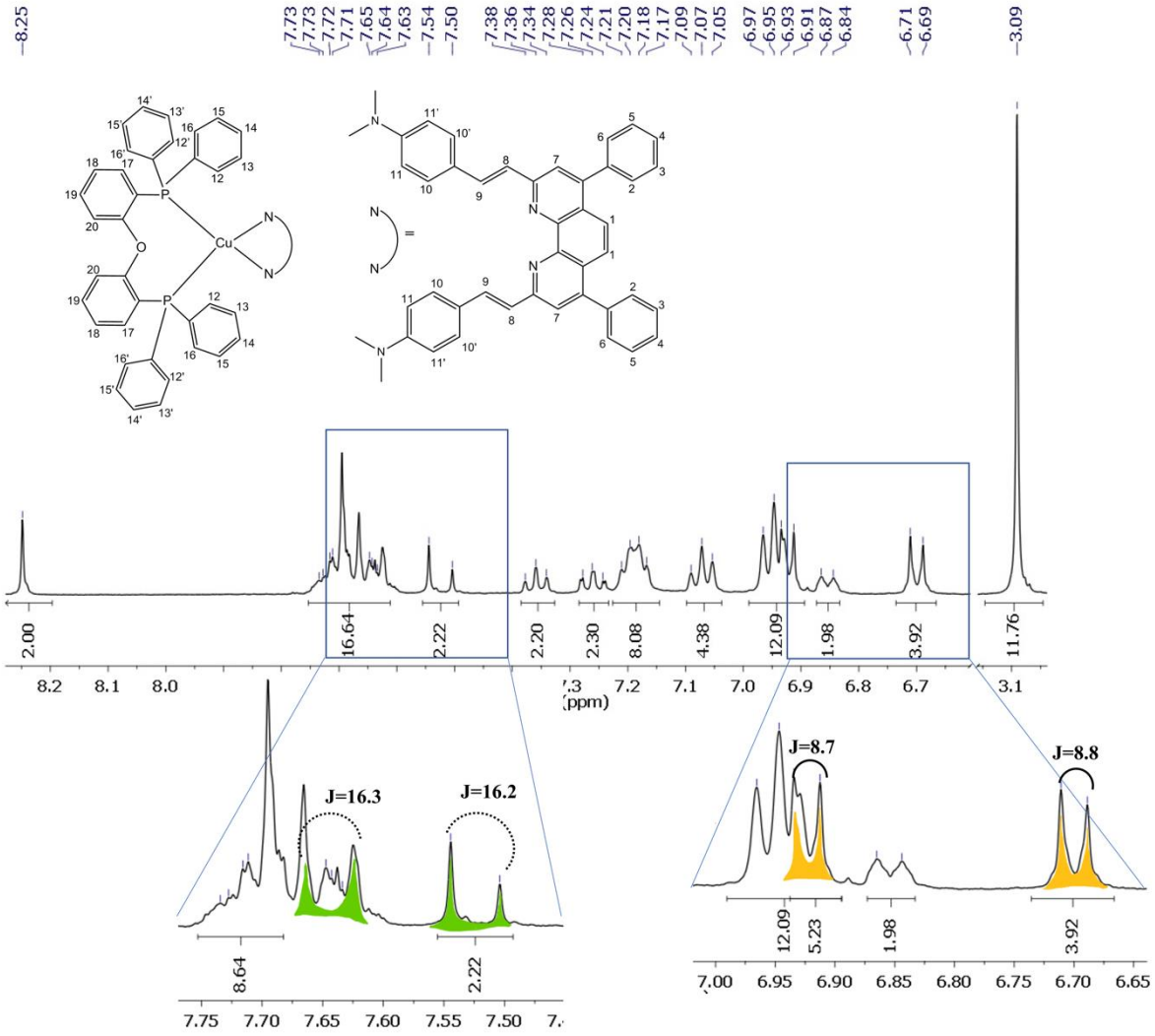

Figure S8. ^{1}H NMR (400 MHz, $(CD_3)_2CO$, 298 K) of **Cu-N^N_b** complex. Inset shows the hydrogen labels are used for the assignation.

^{1}H NMR (400 MHz, $(CD_3)_2CO$) δ 8.25 (s, 2H$_1$), 7.76-7-59 (m, 2H$_2$, 2H$_3$, 2H$_4$, 2H$_5$, 2H$_6$, 2H$_7$, 2H$_{20}$), 7.65 (d, $J_{8\text{-}9}$ = 16.3 Hz, 2H$_8$), 7.52 (d, $J_{8\text{-}9}$= 16.2 Hz, 2H$_9$), 7.36 (t, 2H$_{19}$), 7.26 (t, 2H$_{18}$), 7.19 (dd, 2H$_{12}$, 2H$_{12'}$, 2H$_{16}$, 2H$_{16'}$), 7.07 (t, 2H$_{14}$, 2H$_{14'}$), 6.99-6.90 (m, 2H$_{13}$, 2H$_{13'}$, 2H$_{15}$, 2H$_{15'}$), 6.92 (d, $J_{10\text{-}11}$= 8.7 Hz, 2H$_{10}$, 2H$_{10'}$), 6.85 (d, 2H$_{17}$), 6.70 (d, $J_{11\text{-}10}$ = 8.8 Hz, 2H$_{11}$, 2H$_{11'}$), 3.09 (s, CH_3, 12H).

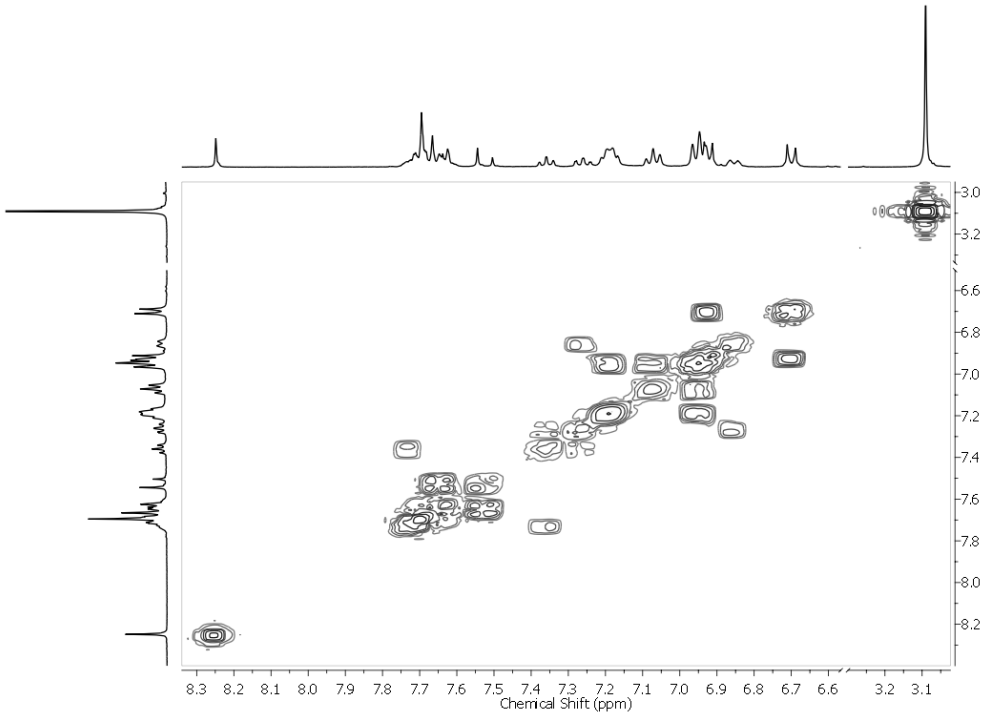

Figure S9. ^{1}H-^{1}H COSY (400 MHz, $(CD_3)_2CO$, 298 K) of **Cu-N^N$_b$** complex.

S4.2 NMR characterizations of Cu-N^N$_b$ complex in CD_3CN

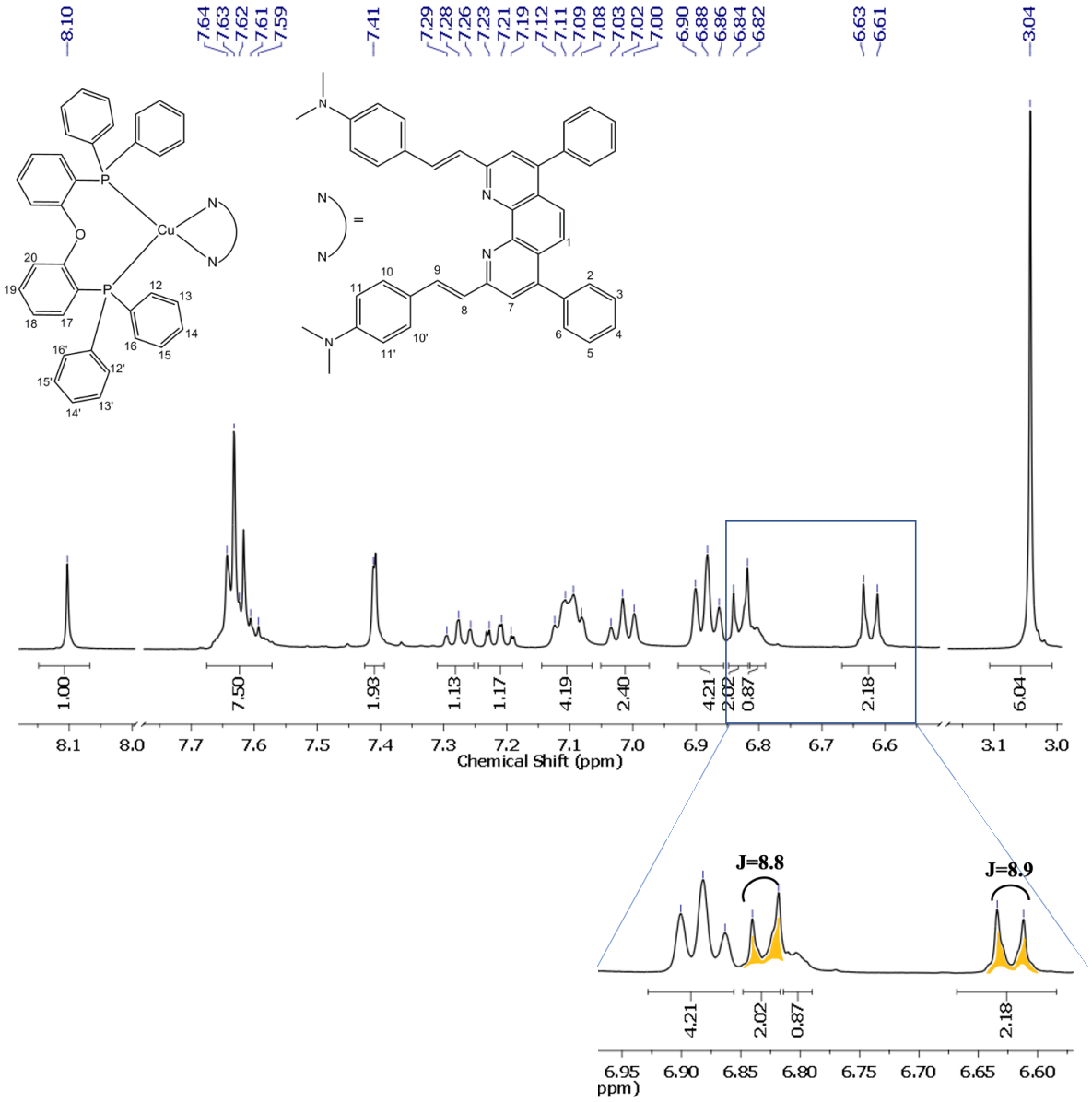

Figure S10. ^{1}H NMR (400 MHz, CD_3CN, 298 K) of **Cu-N^N$_b$** complex. Inset shows the hydrogen labels are used for the assignation.

^{1}H NMR (400 MHz, CD_3CN) δ 8.10 (s, H_1), 7.64-7.59 (m, H_2, H_3, H_4, H_5, H_6, H_7, H_{20}), 7.41 (dt, H_8, H_9), 7.28 (t, H_{19}), 7.21 (td, H_{18}), 7.10 (dd, H_{12}, $H_{12'}$, H_{16}, $H_{16'}$), 7.02 (t, H_{14}, $H_{14'}$), 6.88 (t, H_{13}, $H_{13'}$, H_{15}, $H_{15'}$), 6.83 (d, $J_{10\text{-}11}$ = 8.8 Hz, H_{10}, $H_{10'}$), 6.82 (m, H_{17}), 6.62 (d, $J_{11\text{-}10}$ = 8.9 Hz, H_{11}, $H_{11'}$), 3.04 (s, CH_3, 6H).

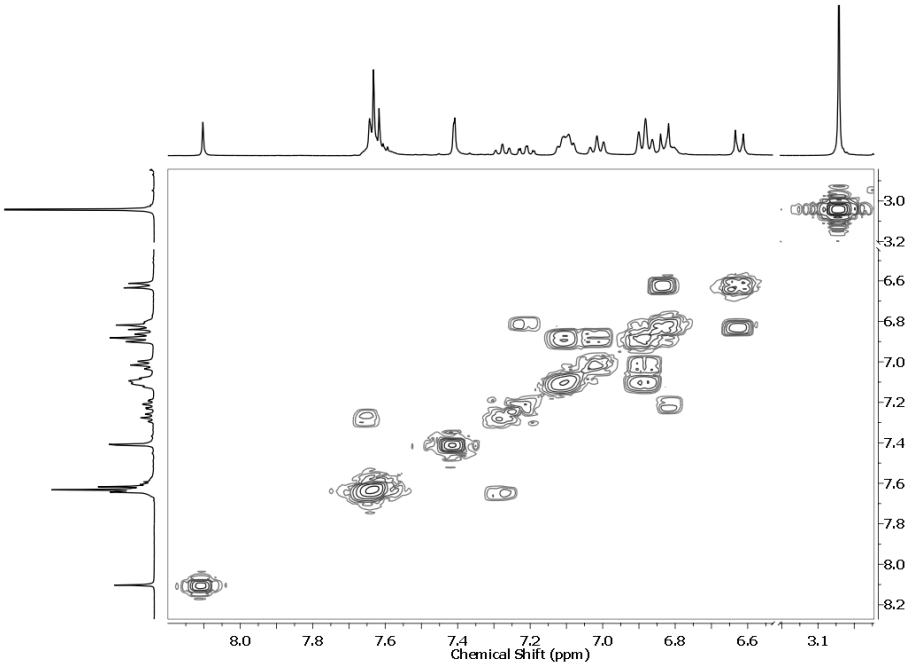

Figure S11. ^{1}H-^{1}H COSY (400 MHz, CD_3CN, 298 K) of **Cu-N^N$_b$** complex.

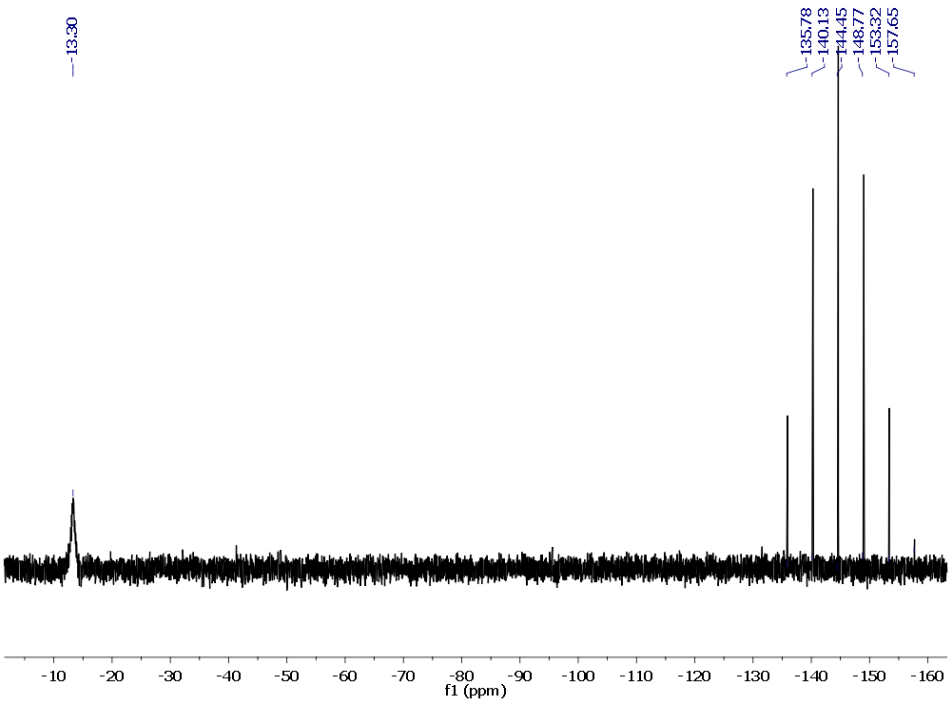

Figure S12. ^{31}P{^{1}H} NMR (162 MHz, CD_3CN, 298 K) of **Cu-N^N$_b$** complex.

^{31}P{^{1}H} NMR (162 MHz, CD_3CN) δ: -13.30 (br s, POP), -144.64 (m, $[PF_6]^-$).

S5. Benchmark study with other DFT functionals

A benchmark study was performed to test the reliability of the selected methodology. The absorption spectra and emission energies were determined for **Cu-N^N$_a$** complex and compared with their experimental data. The absorption spectra were obtained from the optimized geometry in the ground state using the TD-DFT methodology and the T_1 state was fully optimized through TD-DFT optimization with eight different DFT functional: B3LYP,[1] B3PW91,[2-4] BLYP,[5] M06,[6] TPSSH,[7] wB97XD,[8] M06-2X,[6] and PBE0.[9]

The emission energy was calculated as the vertical energy difference between the relaxed triplet state and ground state at the optimized triplet geometry. The implicit solvent effects by the IEF-PCM method were also included using dichloromethane as solvent. The basis set and pseudo-potential used are the same described in the manuscript.

Table S1. Emission wavelengths from the triplet excited states for **Cu-N^N$_a$**.

Functional	**λ_{emi} (nm)**
B3LYP	634
B3Pw91	643
BLYP	916
M06	692
TPSSH	768
wB97XD	726
M06-2X	**555**
PBE0	672
Experimental	*558*[10]

M06-2X functional presents the smallest deviation (3 nm) with respect to the experimental emission energy of **Cu-N^N$_a$** complex, therefore, this functional was selected to describe the emission of **Cu-N^N$_b$**. However, M06-2X functional overestimates the values of the MLCT band (270 to 310 nm) of the absorption spectrum, therefore, PBE0 functional was chosen to reproduce the absorption properties. The MLCT band was determined in a range between 340 and 390 nm which is close to the experimental data (350-450 nm).[10] The choice of two different functionals that allow describing the ground and the excited state is a strategy that has been used in the DFT calculations of compounds with transition metals.[11, 12]

S6. Cyclic voltammetry characterization

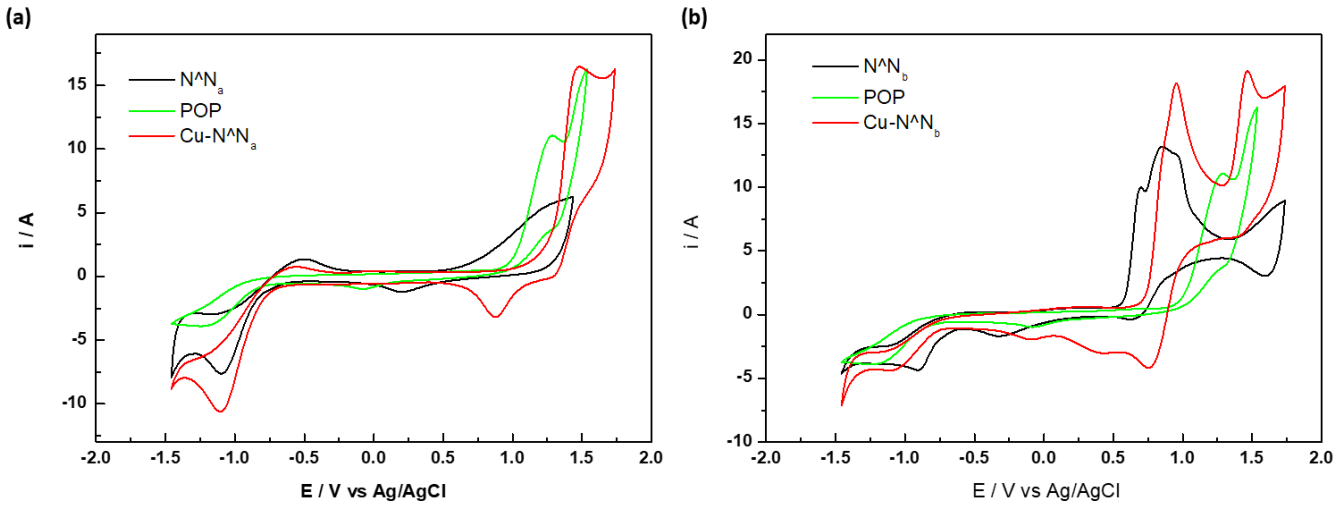

Figure S13. Cyclic voltammograms of (a) **Cu-N^N$_a$**, **N^N$_a$** and **POP** ligands, and (b) **Cu-N^N$_b$**, **N^N$_b$** and **POP** ligands**,** in dichloromethane solution.

S7. Molecular orbitals and structure electronic of the ground state

Table S2. Energy of frontier molecular orbitals (eV) and H-L gaps of the ground state (S_0) obtained at the PBE0/6-31G(d,p)/LANL2DZ level of theory.

Orbital	Cu-N^N_a	Cu-N^N_b	N^N_a	N^N_b
L+2	-1.22	-1.60	-0.39	-1.16
L+1	-2.08	-2.03	-1.41	-1.33
L	-2.22	-2.33	-1.41	-1.83
H	-6.24	-5.38	-6.27	-5.05
H-1	-6.86	-5.52	-6.76	-5.22
H-2	-6.90	-6.25	-6.93	-6.22
H-3	-6.93	-6.67	-7.18	-6.61
Δ H-L	**4.02**	**3.05**	**4.86**	**3.22**

Table S3. Contribution to molecular orbitals (%) of all complexes calculated from HOMO-3 to LUMO+2 in the ground state (S_0), obtained at the PBE0/6-31G(d,p)/LANL2DZ level of theory.

Orbital	Cu-N^N_a			Cu-N^N_b		
	Cu	***P^P***	***N^N***	***Cu***	***P^P***	***N^N***
L+2	1	99	1	0	2	98
L+1	0	1	99	2	2	96
L	2	2	96	0	0	100
H	34	54	12	1	1	98
H-1	31	12	57	0	1	99
H-2	34	15	51	31	51	18
H-3	41	50	9	38	10	52

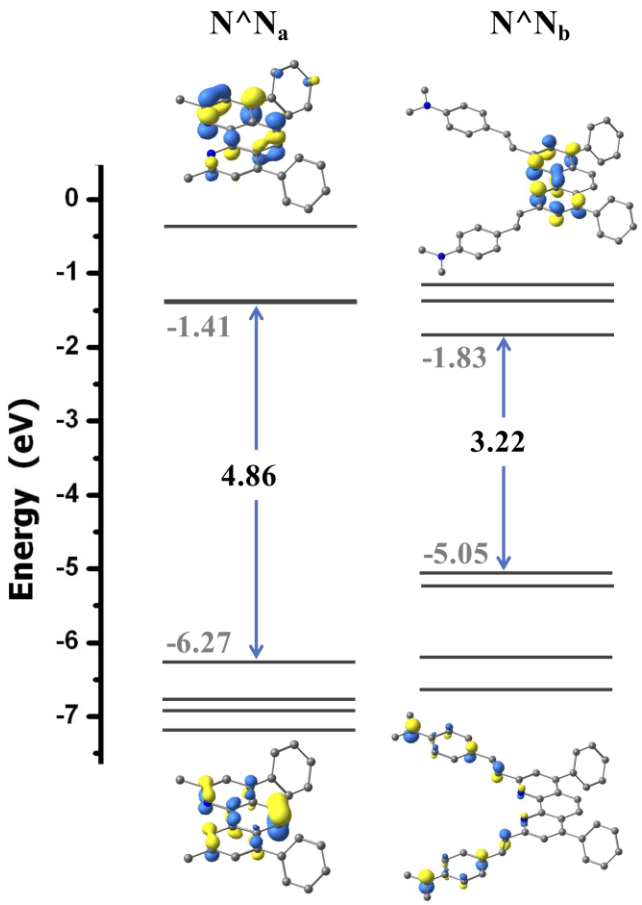

Figure S14. Energy diagram and surfaces of the HOMO and LUMO of ligands: **N^N$_a$** and **N^N$_b$**. Obtained at the PBE0/6-31G(d,p)/LANL2DZ level of theory.

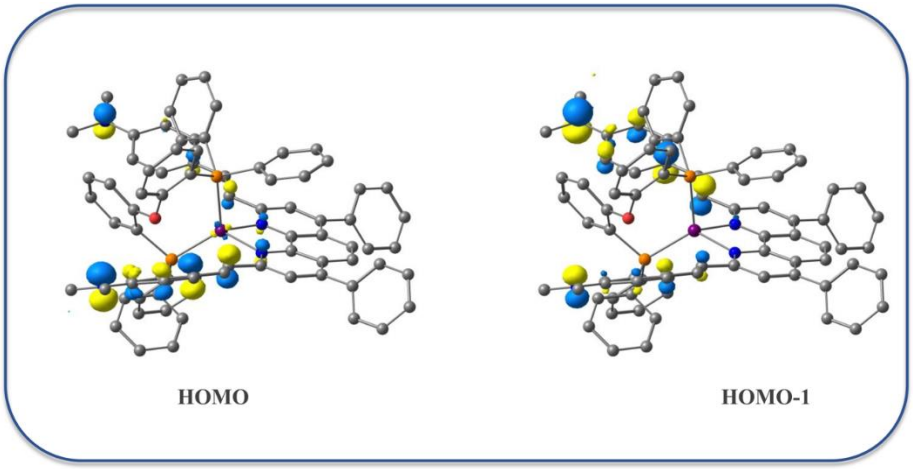

Figure S15. Isosurfaces of the HOMO and HOMO-1 for **Cu-N^N$_b$**. Obtained at the PBE0/6-31G(d,p)/LANL2DZ level of theory.

S8. Luminescence properties

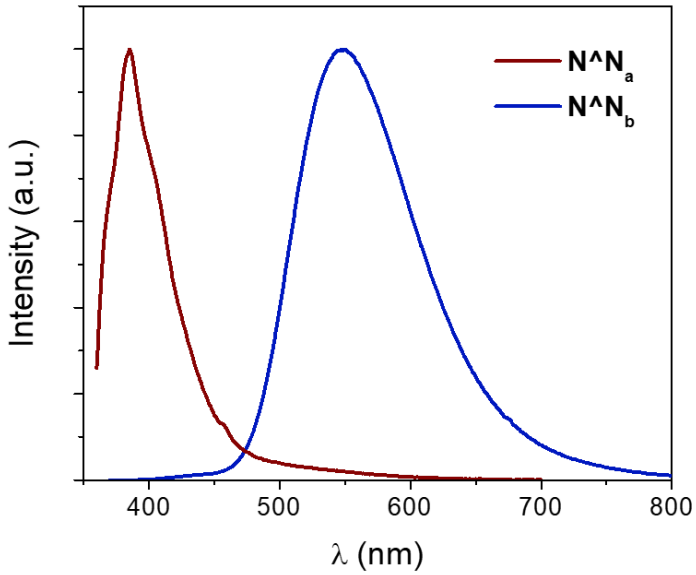

Figure S16. Emission spectra of the **N^N$_a$** and **N^N$_b$** ligands, registered in dichloromethane solution.

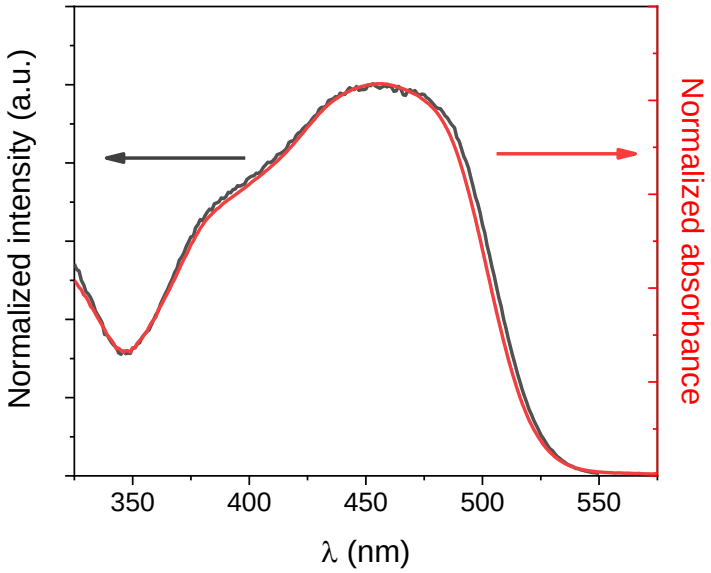

Figure S17. Comparison of the excitation spectrum (recording emission at 580 nm, black trace) and the absorption spectrum (red trace) of **Cu-N^N$_b$** in dichloromethane solution.

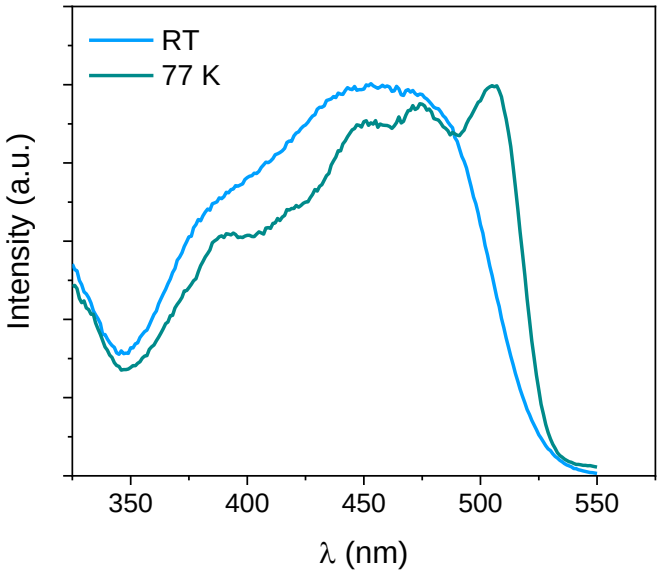

Figure S18. Excitation spectra of **Cu-N^N$_b$** in dichloromethane solution and in a glassy matrix at 77 K (4/1 ethanol/methanol). The structured pattern and red-shift observed at 77 K when compared to room temperature conditions can be related to the effect of the medium and are consistent with the charge transfer nature of the absorption band.

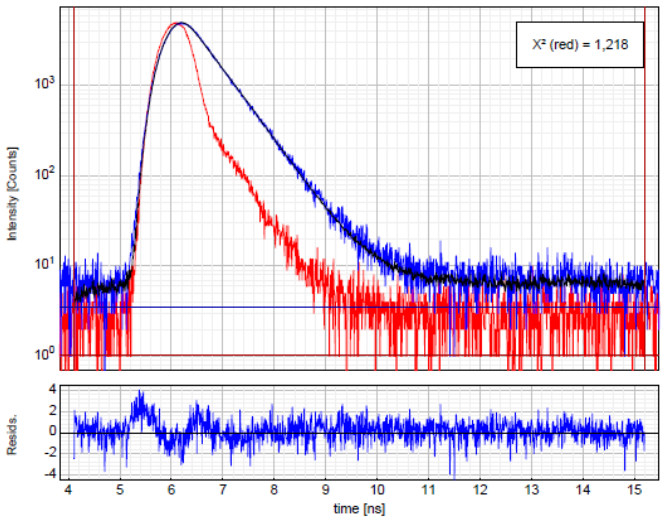

Figure S19. Time-resolved emission decay of **Cu-N^N$_b$** in degassed dichloromethane solution obtained by time-correlated single-photon-counting (excitation at 380 nm, analysis at 565 nm). The fitting provides a lifetime of 0.48 ns.

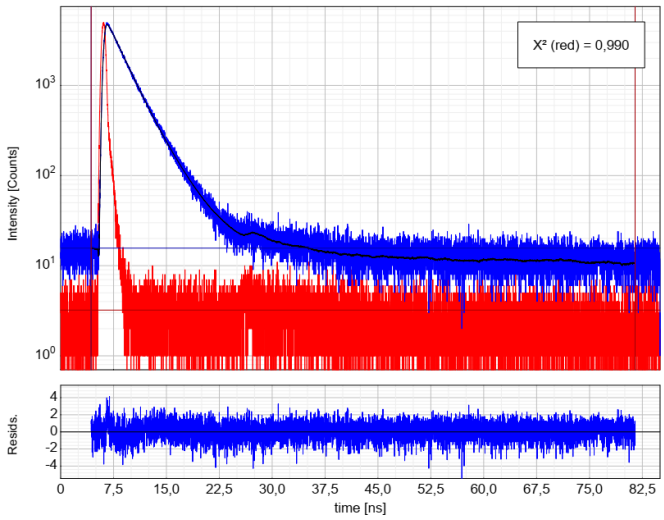

Figure S20. Time-resolved emission decay of **N^N$_b$** in degassed dichloromethane solution obtained by time-correlated single-photon-counting (excitation at 380 nm, analysis at 540 nm). A biexponential fitting has been applied providing two time-constants of 2.24 ns (70%) and 3.82 (30%) corresponding to an average lifetime of 2.71 ns.

S9. Triplet excited states calculated to Cu-N^N$_b$ complex

Table S4. Triplet excited states properties for the **Cu-N^N$_b$**

State	$E_{excitation}$ /eV ($\lambda_{excitation}$/nm)	Main Configuration	Description
T_1	1.412 (878)	L → H (80%)	N^N(π*)→N^N(π); ^{3}ILCT
T_2	1.980 (626)	L → H-1 (44%) L+1 → H (30%)	N^N(π*)→N^N(π); ^{3}ILCT N^N(π*)→N^N(π); ^{3}ILCT
T_3	2.755 (450)	L → H-2 (19%) L+1 → H (14%) L → H-3 (14%)	N^N(π*)→N^N(π)+P^P(π)+Cu(d); ^{3}MLCT/^{3}LLCT/^{3}ILCT N^N(π*)→N^N(π);^{3}ILCT N^N(π*)→N^N(π)+Cu(d); ^{3}MLCT/^{3}ILCT

References

1. A. D. Becke, *The Journal of Chemical Physics*, 1993, **98**, 5648-5652.
2. J. P. Perdew, J. A. Chevary, S. H. Vosko, K. A. Jackson, M. R. Pederson, D. J. Singh and C. Fiolhais, *Physical Review B*, 1992, **46**, 6671-6687.
3. J. P. Perdew, J. A. Chevary, S. H. Vosko, K. A. Jackson, M. R. Pederson, D. J. Singh and C. Fiolhais, *Physical Review B*, 1993, **48**, 4978.
4. J. P. Perdew and K. Burke, *Physical Review B - Condensed Matter and Materials Physics*, 1996, **54**, 16533-16539.
5. B. Miehlich, A. Savin, H. Stoll and H. Preuss, *Chemical Physics Letters*, 1989, **157**, 200-206.
6. Y. Zhao and D. G. Truhlar, *Theoretical Chemistry Accounts*, 2008, **120**, 215-241.
7. X. Shang, D. Han, D. Li, S. Guan and Z. Wu, *Chemical Physics Letters*, 2013, **588**, 68-75.
8. J. D. Chai and M. Head-Gordon, *Physical Chemistry Chemical Physics*, 2008, **10**, 6615-6620.
9. C. Adamo and V. Barone, *Journal of Chemical Physics*, 1999, **110**, 6158-6170.
10. N. Armaroli, G. Accorsi, M. Holler, O. Moudam, J. F. Nierengarten, Z. Zhou, R. T. Wegh and R. Welter, *Advanced Materials*, 2006, **18**, 1313-1316.
11. X. Shang, D. Han, Q. Zhan, D. Zhou and G. Zhang, *New Journal of Chemistry*, 2015, **39**, 2588-2595.
12. Q. Zhang, L. Wang, X. Wang, Y. Li and J. Zhang, *Organic Electronics*, 2016, **28**, 100-110.